

Biomarkers, Genomics, Proteomics, and Gene Regulation

Co-Expression of XIAP and Cyclin D1 Complex Correlates with a Poor Prognosis in Patients with Hepatocellular Carcinoma

Yufang Che,* Fei Ye,[†] Ruliang Xu,[‡] Haitao Qing,*
Xinying Wang,* Fei Yin,[†] Miao Cui,*
David Burstein,[†] Bo Jiang,* and David Y. Zhang,[†]

From the Guangdong Provincial Key Laboratory of Gastroenterology,* Department of Gastroenterology, Nanfang Hospital, Southern Medical University, Guangzhou, China; the Department of Pathology,[†] Mount Sinai School of Medicine, New York, New York; and the Department of Pathology,[‡] New York University School of Medicine, New York, New York

Hepatocellular carcinoma (HCC) is one of the most common malignant tumors in the world. Despite improved diagnosis and treatment, the prognosis for HCC patients remains poor. The goal of this study was to identify key regulatory proteins and signaling pathways important for cell apoptosis and proliferation as biomarkers for prognostication and targeted therapy. Protein Pathway Array was applied to screen 38 signaling proteins and phosphoproteins in 12 paired HCC tumors and surrounding benign tissues and found that 20 of them, including XIAP, CDK4, CDK6, and Cyclin D1, were overexpressed in HCC tissues. Immunostaining results of XIAP, CDK4, and Cyclin D1 in an additional 59 HCC tissues showed that the expression of XIAP correlated with the expression of CDK4/Cyclin D1, and that the increased expression of these proteins correlated with poor overall survival in these patients. Further studies using the HCC Huh7 cell line transfected with XIAP siRNA or expression vector demonstrated that XIAP regulated the expression of CDK4, CDK6, and Cyclin D1 via NF- κ B and PTEN pathways. Finally, inhibition of XIAP using embelin, a XIAP-specific small molecule, leads to an increased apoptosis and decreased cell proliferation via arrest at G1 phase. Taken together, XIAP is a central modulator regulating cell apoptosis and cell cycle progression. Therefore, XIAP together with cell cycle regulatory proteins can be used as prognostic markers and therapeutic targets. (*Am J Pathol* 2012, 180: 1798–1807; DOI: 10.1016/j.ajpath.2012.01.016)

Hepatocellular carcinoma (HCC) ranks as the fifth most common malignancy and the third leading cause of cancer death in the world, being responsible for 80% of primary malignant liver tumors in adults.¹ HCC has a 5-year relative survival rate of approximately 7% and causes more than 600,000 deaths annually worldwide.² Although its prevalence is highest in Africa and Asia, its incidence in western countries is rising, mainly due to increasing rates of alcoholic liver diseases and hepatitis C infection.³ Currently, there is no effective treatment of HCC except surgical resection and liver transplantation for early-stage cancer. However, fewer than 15% of patients undergo surgery, because of late clinical presentation and diagnosis.⁴ Therefore, the development of new therapeutic targets and biomarkers is urgently needed for early detection of HCC via understanding the molecular signaling pathways important in HCC carcinogenesis.

Although the underlying molecular mechanism of HCC carcinogenesis remains largely unknown, it is clear that the imbalance between survival and apoptotic signals is critical in HCC initiation and progression. Lines of evidence suggest that several signaling pathways important for cell proliferation and survival are activated in HCC, including the Ras/Raf/MEK/ERK pathway, the PI3k/AKT/mTOR pathway, and the Wnt/ α -catenin pathway.^{5,6} Furthermore, overexpression of positive cell cycle regulators such as Cyclin D, Cyclin E, Cyclin A, and CDKs has been reported in HCC, suggesting enhanced cell proliferation.^{5,7} Altered apoptotic pathways are also observed in HCC. For example, antiapoptotic proteins, such as XIAP, are overexpressed in a great percentage of HCC cases.⁸ Conversely, proapoptotic proteins, such as Bax or

Supported in part by a grant from Science and Technology Planning Project of Guangdong Province 2009B030801213 (B.J.).

Accepted for publication January 10, 2012.

Address reprint requests to Bo Jiang, M.D., Ph.D., Guangdong Provincial Key Laboratory of Gastroenterology, Department of Gastroenterology, Nanfang Hospital, Southern Medical University, Guangzhou, Guangdong, China 510515 or David Y. Zhang, M.D., Ph.D., Department of Pathology, Mount Sinai School of Medicine, New York, NY 10029. E-mail: drjiang@163.com or david.zhang@mssm.edu.

Bcl-X_s, are down-regulated in HCC; in addition, dysfunction of p53, PTEN, and Smad has been observed due to mutations in these genes.⁵ However, it is not clear how proliferation and apoptotic pathways work together to confer HCC growth.

Therefore, in our study, we examined the levels of expression and phosphorylation of important proteins involved in cell proliferation, apoptosis, and cell cycle progression in HCC using our newly developed Protein Pathway Array (PPA) technology. We demonstrate significant cross talk between cell cycle progression and apoptosis in HCC via the central regulatory protein XIAP. This finding will be helpful in the future development of effective anti-HCC therapies.

Materials and Methods

Reagents and Antibodies

Embelin (catalog no. 550243) and α -actin (catalog no. A5316) were obtained from Sigma (St. Louis, MO). Antibodies specific to XIAP (catalog no. 610763) and ERK 1/2 (catalog no. 612359) were purchased from Becton Dickinson (Franklin Lakes, NJ). Antibodies specific to CDC2p34 (catalog no. sc-54), CDK2 (catalog no. sc-163), CDK4 (catalog no. sc-260), CDK6 (catalog no. sc-177), Cyclin D1 (catalog no. sc-718), p27 (catalog no. sc-528), 14-3-3- α (catalog no. sc-628), α -tubulin (catalog no. sc-5286), neuropilin (catalog no. sc-5541), Bax (catalog no. sc-493), BCL2 (catalog no. sc-7382), p53 (catalog no. sc-126), CDC25B (catalog no. sc-5619), CDC25C (catalog no. sc-327), Cyclin B1 (catalog no. sc-594), Cyclin E (catalog no. sc-481), Wee1 (catalog no. sc-325), PCNA (catalog no. sc-56), BRCA1 (catalog no. sc-642), CHK1 (catalog no. sc-8408), MDM2 (catalog no. sc-965), PKC α (catalog no. sc-208), EGFR (catalog no. sc-03), ETS1 (catalog no. sc-350), c-MYC (catalog no. sc-40), E2F-1 (catalog no. sc-251), GATA 1 (catalog no. sc-266), GATA 2 (catalog no. sc267), HIF-1 α (catalog no. sc-10790), Trap (catalog no. sc-28204), and Ki-67 (catalog no. sc-7844) were purchased from Santa Cruz (Santa Cruz, CA). Specific antibodies, including p-GSK-3 α / β (Ser 21/9) (catalog no. 9331), α -catenin (catalog no. 9562), and AKT (catalog no. 9272) were purchased from Cell Signaling Technology (Danvers, MA). COX-2 (catalog no. 160107), HSP90 (catalog no. SPA-830), HIF-2 α (catalog no. NB100-122), and HIF-3 α (catalog no. ab10134) were obtained from Cayman, Stressgen, Novus, and Abcam, respectively. Goat anti-rabbit (catalog no. 170-6515) and goat anti-mouse (catalog no. 172-1011) HRP conjugate antibodies, were purchased from Bio-Rad (Hercules, CA). Membrane-blocking agent and bovine serum albumin (BSA) were purchased from Amersham (Buckinghamshire, United Kingdom) and Sigma (St. Louis, MO), respectively.

HCC Tissue Samples and PPA Analysis. Liver tissue samples, including the malignant and surrounding benign tissues, were obtained from 12 HCC patients who underwent surgical resection at Nanfang Hospital, Guangzhou, China. The tissue samples were frozen on

dry ice within 20 minutes of collection and stored at -70°C . A section of tissue (3 mm in diameter) was homogenized in lysis buffer containing 20 mmol/L Tris-HCl (pH 7.5), 20 mmol/L sodium pyrophosphate, 40 mmol/L β -glycerophosphate, 30 mmol/L sodium fluoride, 2 mmol/L EGTA, 100 mmol/L NaCl, 1 mmol/L Na₃VO₄, 0.5% NP-40, 1 \times protease inhibitors (Roche Applied Science, Indianapolis, IN), and 1 \times phosphatase inhibitor cocktail (Roche Applied Science, Indianapolis, IN). The homogenate was sonicated three times for 15 seconds and then subjected to ultracentrifugation at 100,000 $\times g$ for 30 minutes. The protein concentration was determined using a BCA Protein Assay kit (Pierce, Rockford, IL).

The protein extract (350 μg /sample) was loaded into one well across the entire width of a 10% SDS-polyacrylamide gel and separated by electrophoresis as described previously.^{9,10} After electrophoresis, the proteins were transferred electrophoretically to a nitrocellulose membrane (Bio-Rad) that was then blocked for 1 hour with blocking buffer including either 5% milk or 3% BSA in 1 \times TBST containing 20 mmol/L Tris-HCl (pH 7.5), 100 mmol/L NaCl, and 0.1% Tween-20. Next, the membrane was clamped onto a Western blotting manifold (Mini-PROTEAN II Multiscreen apparatus, Bio-Rad) that isolates 20 channels across the membrane. The multiplex immunoblot was performed using a total of 38 protein-specific or phosphorylation site-specific antibodies. A mixture of one to two antibodies in the blocking buffer was added to each channel and then incubated at 4 $^{\circ}\text{C}$ overnight. The membrane was then washed with 1 \times TBS and 1 \times TBST, and then further incubated with secondary anti-rabbit or anti-mouse antibody conjugated with HRP (Bio-Rad) for 1 hour at room temperature. The membrane was developed with chemiluminescence substrate (Immun-Star HRP Peroxide Buffer/Immun-Star HRP Luminol Enhancer, Bio-Rad), and chemiluminescent signals were captured using the ChemiDoc XRS System (Bio-Rad). The same membrane was then stripped using stripping buffer (Restore Western blot stripping buffer, Thermo Scientific, Rockford IL) and then used to detect a second set of primary antibodies as described above. The signals of each protein were determined by densitometric scanning (Quantity One software package, Bio-Rad). Differences in protein levels were determined by measuring the density of each band and normalized using internal standards.

Immunohistochemistry

Formalin-fixed, paraffin-embedded tissue samples from 59 primary human HCCs were randomly selected from achieved tissue bank. The study was performed in accordance with the institutional ethical guidelines and was approved by the medical ethics committee of Southern Medical University. Informed consent was obtained from all patients.

The immunohistochemical methods have been described previously.¹¹ Sections were incubated with primary antibodies in appropriate dilutions overnight at 4 $^{\circ}\text{C}$ (XIAP antibody, 1:100 dilution; Cyclin D1 antibody, 1:100 dilution; CDK4 antibody, 1:100 dilution). Scoring of tissue

slides was performed independently by two investigators (Y.C. and D.Y.Z.) based on both staining intensity and extent of expression across the section. Intensity of staining was scored as 0 (negative), 1 (weak), or 2 (strong). The extent of staining was based on the percentage of positive tumor cells: 0 (negative), 1 (1% to 25%), 2 (26% to 50%), 3 (51% to 75%), and 4 (76% to 100%). The final score of each sample was assessed by adding the results of the intensity and extent of staining. Therefore, each case was finally considered as low expression if the final score 0 to 1 (–) or 2 to 3 (+), and high expression if the final score was 4 to 5 (+) or 6 to 7 (++) , respectively (17).

Cell Treatment with Embelin and PPA Analysis

Human HCC cell lines HepG2/2.2.1 and Huh7 were purchased from the American Type Culture Collection (Manassas, VA). The cells were maintained in Minimum Essential Medium (GIBCO, Carlsbad, CA) supplemented with 10% fetal bovine serum (Invitrogen, Carlsbad, CA) and 1% penicillin/streptomycin (Fisher Scientific) or Dulbecco's modified Eagle's medium Nutrient Mixture F-12 (GIBCO, Carlsbad, CA) supplemented with 10% fetal bovin serum and 1% sodium pyruvate (Fisher Scientific, Pittsburgh, PA) at 37°C in a humidified atmosphere of 5% CO₂. For treatment with embelin, cells were incubated in complete medium in the presence of embelin at the different concentrations. The proteins from Huh7 cells treated with 25 μmol/L embelin for 24 hours were extracted, and the protein expression levels were determined using PPA as described above.

Cell Viability Assay

The cell viability assay was performed using CellTiter-Glo Luminescent Cell Viability Assay according to the manufacturer's instructions (Promega, Madison, WI). After treatment with embelin, a 100-μl quantity of cells was transferred into each well of a 96-well, opaque white plate. For control wells, 100 μl of culture medium without cells was used to obtain background luminescence. A 100-μl quantity of CellTiter-Glo Reagent was added to each well and mixed for 2 minutes on a Rotary Shaker I (Diagen Corporation, Rutherford, NJ) to induce cell lysis. The luminescence of each sample was measured in a plate by a DIAGEN DML 2000 illuminometer (Diagen Corporation, Rutherford, NJ) after incubation at room temperature for 10 minutes to stabilize the luminescence signal.

Cell Cycle Analysis

Cells were collected and washed with PBS, then suspended in a propidium iodide solution containing 100 μg/mL of propidium iodide, 0.1% (v/v) Triton X-100, and 100 μg/mL of RNase A in 1× PBS. After incubation in the dark for 30 minutes at room temperature, the samples were analyzed by flow cytometry (Becton Dickinson, San Jose, CA). Cell cycle phase distribution

was determined using Modfit Software (Verity Software House, Topsham, ME).

Apoptosis Analysis

Apoptosis analysis was performed using an Annexin-V-FLUOS Staining Kit (Roche Applied Science, Indianapolis, IN). The samples (10⁶ cells/sample) were washed with PBS and resuspended in 100 μl of Annexin-V-FLUOS labeling solution for 10 to 15 minutes at room temperature. The cells were analyzed by flow cytometry (Becton Dickinson), and data were analyzed using the Cell Quest program (Becton Dickinson).

Transfections of XIAP siRNA and Expression Vector

Human pDsRed-XIAP expression vector and empty vector were kindly provided by Dr. Jide Wang (Nangfang Hospital, Guangzhou, China). Human XIAP siRNA was designed and synthesized by Qiagen (Doncaster, Victoria, Australia). Double-stranded XIAP siRNA sequences were 5'-GGAGAUACCGUGCGGUGCdTdT-3' (forward) and 5'-AGCACCGCACGGUAUCUCCdTdT-3' (reverse).¹² Positive control siRNA (GAPDH) and negative control siRNA (scramble RNA) were purchased from Ambion (Austin, TX). For transfection of the expression vectors, Huh7 cells were seeded at a density of 0.5 × 10⁵ cells in 24-well culture plates (Corning, NY) and incubated at 37°C for 24 hours to allow cells to reach 90% to 95% confluence. Transfections were performed using 0.8 μg XIAP vector or empty vector as control with Lipofectamine 2000 (Invitrogen, Carlsbad, CA) following the manufacturer's instructions. After a 6-hour transfection, the cells were incubated in fresh medium for an additional 48 hours. For transfection of siRNAs, Huh7 cells were seeded in 24-well culture plates as described above. The transfections were performed with 150 μmol/L XIAP siRNA duplex, 150 μmol/L GAPDH siRNA duplex, or 150 μmol/L negative control siRNA (scramble) in Huh7 cells using X-temenGENE siRNA Transfection Reagent (Roche Applied Science, Indianapolis, IN) following the manufacturer's instructions. After a 24-hour transfection, the cells were incubated in fresh medium for an additional 48 hours.

RT-PCR Analysis

Total cellular RNA was extracted from cells using the RNeasy Mini Kit (Qiagen, Doncaster, Victoria, Australia) according to the manufacturer's instructions. The first-strand cDNA was synthesized from 5 μl of total RNA using the SuperScript III First-Strand Synthesis System for RT-PCR Kit (Invitrogen, Carlsbad, CA), following the manufacturer's instructions. PCR amplification was performed with the following gene-specific primers: human GAPDH 5'-TGATGACATCAAGAAGGTGGTGAAG-3' (forward), 5'-TCCTTGGAGCCATGTGGGCCAT-3' (reverse) (BIOMOL Research Laboratories Inc. Butler Pike, PA)¹³; human XIAP 5'-GGTTCAGTTTCAAGGACATT-3'

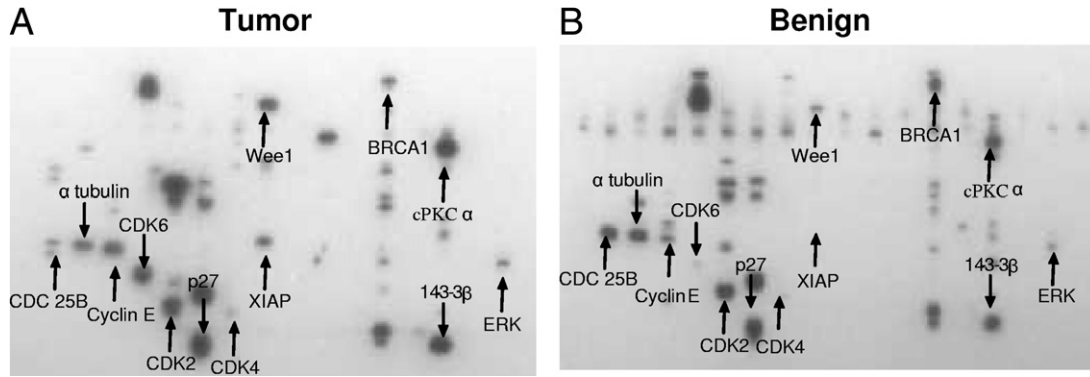


Figure 1. Representative autoradiographs showing expression and phosphorylation of the functionally important regulatory proteins in paired tumor (A) and benign (B) tissues detected by PPA.

(forward), 5'-CAAGGAACAAAAACGATAGC-3' (reverse).¹⁴ The conditions for PCR amplification were as follows: one cycle of 5 minutes at 95°C, 30 cycles of (30 seconds at 95°C, 30 seconds at 55°C, and 30 seconds at 72°C), and one cycle of 2 minutes at 72°C for GAPDH; one cycle of 5 minutes at 95°C, 30 cycles of (30 seconds at 94°C, 30 seconds at 56°C, and 30 seconds at 72°C), and one cycle of 5 minutes at 72°C for XIAP.¹⁴ The PCR products were analyzed by electrophoresis on a 2% agarose gel containing ethidium bromide.

Western Blot Analysis

The proteins were extracted from the cells and separated by 10% SDS-PAGE. The membrane was blocked for 20 minutes in TBST containing 5% nonfat dry milk. Antibodies were added to the blot and allowed to bind to the proteins overnight. The blot was washed and incubated with secondary antibody for 1 hour. The membrane was washed and developed for chemiluminescence using the ECL Western blotting analysis system (Bio-Rad). Chemiluminescence signals were captured using the Chemi-Doc XRS System.

Signaling Network Analysis

The protein-protein interaction network was created using Ingenuity Pathway Analysis (IPA; Redwood City, CA). Differentially expressed proteins identified by PPA were imported to the IPA for functional analysis of the network. Based on the Ingenuity Pathway Knowledge database for interactions (known from the literature), the IPA program searched already known interactions among the uploaded proteins and generated a network between these proteins.

Statistical Analysis

Comparisons of quantitative data were analyzed by Student's *t*-test between two groups or by a one-way analysis of variance for multiple groups. Nonparametric Mann-Whitney and Kruskal-Wallis tests were applied to test the significance of differences among groups of clinicopathological parameters. Kaplan-Meier and log-

rank tests were used for overall survival analysis. The level of significance was defined as $P < 0.05$. All analyses were performed with SPSS 13.0 software (SPSS Inc., Chicago, IL).

Results

Differential expression of protein and phosphoproteins in HCC. Twelve pairs of HCC and surrounding tissues were assessed for the expression of proteins and phosphorylation level using PPA (Figure 1). Of 38 antibodies tested, 23 proteins and phosphoproteins were detected, and 20 of them were differentially expressed between benign and malignant tissues (>2-fold; Figure 2). Of the tumors, 54% had increased expression of XIAP, and 46% had increased expression of CDK6. Interestingly, 46% of tumor tissues had increased expression of both XIAP and CDK6. Similarly, 8% of tumors had increased expression of XIAP, Cyclin D1, and CDK4. These findings suggest that these differentially expressed proteins, especially XIAP, Cyclin D1, CDK4, and CDK6, may play important roles in HCC carcinogenesis. Furthermore, co-expression of XIAP with Cyclin D1/CDK4/CDK6 suggests a regulatory relationship between XIAP and Cyclin D1/CDK4/CDK6.

Co-expression of XIAP and Cyclin D1/CDK4 is correlated with a poor prognosis in HCC patients. To further confirm the co-expression of XIAP with Cyclin D1/CDK4,

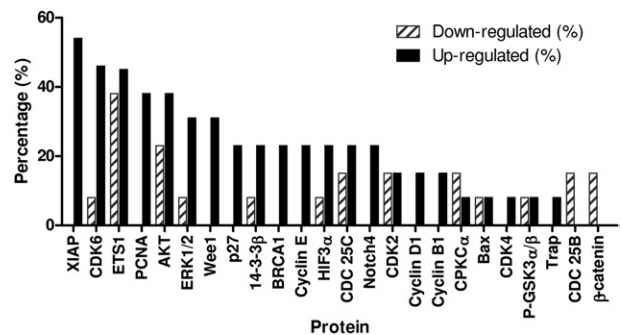


Figure 2. Percentage of up- and down-regulated proteins in tumor tissues. Levels of proteins and phosphoproteins in HCC were compared with those of surrounding tissues, and percentages of each protein with up- or down-regulation in tumors are presented.

Table 1. Profiles of Patients with XIAP-, cdk4-, cyclin D1-Positive or XIAP-, cdk4-, cyclin D1-Negative Hepatocellular Carcinoma

Clinicopathological	Variables	XIAP			Cdk4			cyclin D1		
		Low	High	<i>P</i> value*	Low	High	<i>P</i> value*	Low	High	<i>P</i> value*
Sex	Male	21	34	1.000	22	33	1.000	15	40	1.000
	Female	1	3		2	2		1	3	
Age (years)	≤60	18	32	0.715	20	30	1.000	13	37	0.692
	>60	4	5		4	5		3	6	
Tumor no.	Solitary	20	29	0.294	21	28	0.506	14	35	0.713
	Multiple	2	8		3	7		2	8	
Maximal tumor size (cm)	≤5	8	13	1.000	12	9	0.106	8	13	0.124
	>5	14	24		13	25		7	31	
AFP (ng/mL)	≤60	8	9	0.239	10	7	0.086	5	12	1.000
	>20	28	14		14	28		11	31	
Liver cirrhosis	Absent	10	12	0.406	7	15	0.412	7	15	0.770
	Present	12	25		17	20		10	27	
HBV	Absent	4	13	0.237	4	13	0.143	4	13	0.759
	Present	18	24		20	22		12	30	
HCV	Absent	10	18	1.000	14	14	0.193	11	17	0.077
	Present	12	19		10	21		5	26	
Tumor differentiation	Well	2	15	0.038*	5	10	0.025*	2	13	0.014*
	Moderate	10	13		16	10		12	14	
	Poor	3	16		4	14		2	16	
pTNM stage [†]	I	1	0	0.192	1	0	0.030*	1	0	0.009*
	II	18	26		18	26		10	34	
	III	1	8		1	8		1	8	
	IV	2	3		4	1		4	1	

*Statistical analyses were conducted with Fisher's exact test for all parameters. *P* < 0.05 was considered statistically significant.

[†]The pTNM classification for HCC was based on the American Joint Committee on Cancer/International Union Against Cancer staging system (6th edition, 2002).

59 HCC tissues were obtained from patients who underwent tumor resection at Nanfung hospital, Guangzhou, China. The patients were followed up between 1 and 110 months (median, 14 months). The demographic information of this patient cohort is presented in Table 1. The expression of XIAP, Cyclin D1, and CDK4 in HCC tissues was determined by immunohistochemical stain (Figure 3). CDK6 was not examined because of the poor affinity of the antibody on formalin-fixed tissues.

The IHC results confirmed our initial PPA results, that is, a high level expression of XIAP (62.7%), CDK4 (59.3%), and Cyclin D1 (72.8%) in HCC tissues. Furthermore, based on Spearman's correlation analysis, a high level of expression of XIAP was correlated with a high level of expression of Cyclin D1 and CDK4 (*P* = 0.02) in HCC, further suggesting a connection between XIAP and CDK4/Cyclin D1. Moreover, a high level of expression of Cyclin D1 was also correlated with a high level of expression of CDK4 (*P* < 0.01) in HCC, supporting the notion that Cyclin D1 and CDK4 form a complex to promote HCC proliferation. Univariate analysis of the expression of these proteins with clinical parameters, including age, sex, tumor number, maximal tumor size, AFP level, cirrhosis, tumor differentiation, and TNM stage, demonstrated that the high level expression of these proteins correlates only with poor tumor differentiation (*P* < 0.05) and high TNM stage (except XIAP; *P* < 0.05; Table 1).

The expression levels of these proteins were also correlated with prognosis in HCC patients. Patients with high XIAP expression had significantly lower overall survival compared with those with low XIAP expression (*P* = 0.004; Figure 4A). The 3-year overall survival was 68.2%

for those with low XIAP expression and only 27.0% for those with high XIAP expression. Similarly, lower overall survival rates were observed in patients with high-level expression of CDK4 and Cyclin D1 compared with patients with low-level expression (*P* < 0.001; Figure 4, B and C). The 3-year overall survival rates were 70.8% for groups with low CDK4 expression, 22.9% for groups with high CDK4 expression, 93.8% for groups with low Cyclin D1 expression, and 23.3% for groups with high Cyclin D1 expression.

Based on the expression patterns of XIAP and CDK4 or Cyclin D1, the tumors were separated into six groups (Figure 5): concomitant low expression of XIAP and CDK4 (Group 1) or Cyclin D1 (Group 2), concomitant high expression of XIAP and CDK4 (Group 5) or Cyclin D1 (Group 6), and divergent expression of XIAP and CDK4 (Group 3) or Cyclin D1 (Group 4; ie, high XIAP versus low CDK4 or Cyclin D1 and low XIAP versus high CDK4 or Cyclin D1). Concomitant expression of XIAP and CDK4 (Groups 1 and 5) was found in 41 of 59 tumors (Figure 5A), and concomitant expression of XIAP and Cyclin D1 (Groups 2 and 6) was found in 37 of 59 tumors (Figure 5B). The overall survival rates among these groups were significantly different: Groups 1 and 2 had significantly better survival rates than Groups 5 and 6 (Figure 5, A and B). The 3-year survival rates were 90.0% for low XIAP and low CDK4 expression (Group 1), 66.7% for divergent XIAP and CDK4 expression (Group 3), and 12.9% for high XIAP and high CDK4 expression (Group 5). Similarly, the 3-year survival rates were 83.3% for low XIAP and low CDK4 expression (Group 2), 54.5% for divergent XIAP and CDK4

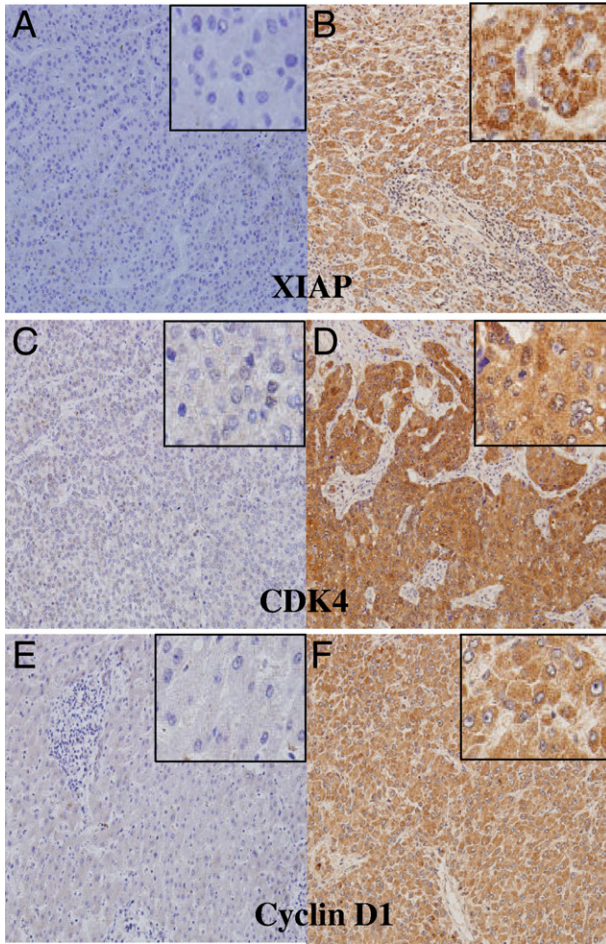


Figure 3. Representative images of immunohistochemical staining of XIAP, CDK4, and Cyclin D1 in HCC tissues. **A** and **B**: Low and high XIAP expression, respectively. **C** and **D**: Low and high expression of CDK4, respectively. **E** and **F**: Low and high Cyclin D1 expression, respectively. Original magnification: $\times 200$ (all images); $\times 400$ (insets).

expression (Group 4), and 12.0% for high XIAP and high CDK4 expression (Group 6).

Effects of embelin on HCC cell proliferation and apoptosis. Embelin is a specific inhibitor of XIAP, which is a key protein that inhibits the activation of caspases 3, 7, and 9. To understand the role of XIAP in HCC growth, HepG2/2.2.1 and Huh7 cells were treated with various concentrations of embelin for 24, 48, and 72 hours, and the number of viable cells were determined using the CellTiter-Glo Luminescent Cell Viability Assay as described above. Our results showed that the number of viable cells decreased with increasing amounts of embelin and incubation time, suggesting an effective inhibition of HCC growth (Figure 6). The 50% inhibitory concentration (IC_{50}) at 24 hours was 35 $\mu\text{mol/L}$ for HepG2/2.2.1 cells and 25 $\mu\text{mol/L}$ for Huh7 cells. Apparently, Huh7 cells are more sensitive to embelin than HepG2/2.2.1 cells.

To understand further the mechanism of growth inhibition by embelin, we analyzed cell cycle phase distribution of Huh7 cells after treatment with embelin, because Huh7 cells are more sensitive to embelin than are HepG2/2.2.1 cells. Our results showed that embelin significantly

blocked Huh7 cell growth at G1 phase with concomitant decreases of G2 and S phases (Figure 7). The percentages of cell arrest at G1 phase increased from 63.41% in control cells to 72.94% in cells treated with 25 $\mu\text{mol/L}$ embelin ($P < 0.01$). The effects of embelin on apoptosis were also evaluated using Annexin V-specific antibodies, and our results showed that apoptotic cell number increased with increasing embelin concentrations (Figure 8). The percentage of apoptotic cells increased from 1.1% in control cells to 11.0% in treated cells ($P < 0.01$; Figure 8), suggesting that embelin suppresses cell proliferation by arresting cell at G1 phase and promotes cells entering into apoptosis.

Regulation of the expression of CDK4/6 and Cyclin D1 by XIAP. Our results showed that CDK4/6 and Cyclin D1 were overexpressed in HCC, regulating the progression from G1 to S phase. Therefore, the expression levels of

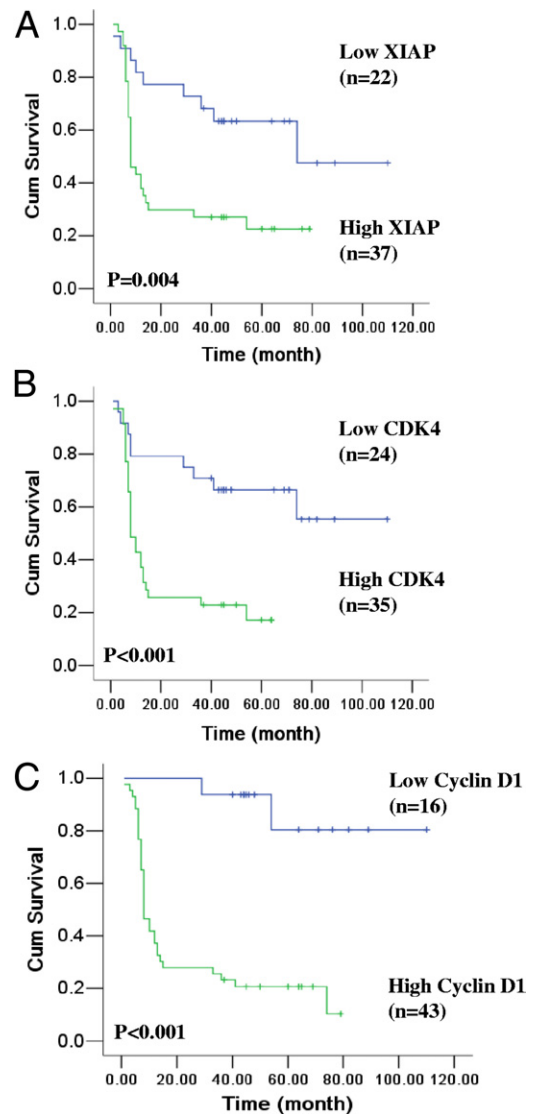


Figure 4. High-level expression of XIAP, CDK4, and Cyclin D1 correlate with unfavorable survival. Overall survival rates of 59 HCC patients who underwent liver tumor resection were compared between high- and low-XIAP groups (**A**), high- and low-CDK4 groups (**B**), and high- and low-Cyclin D1 groups (**C**).

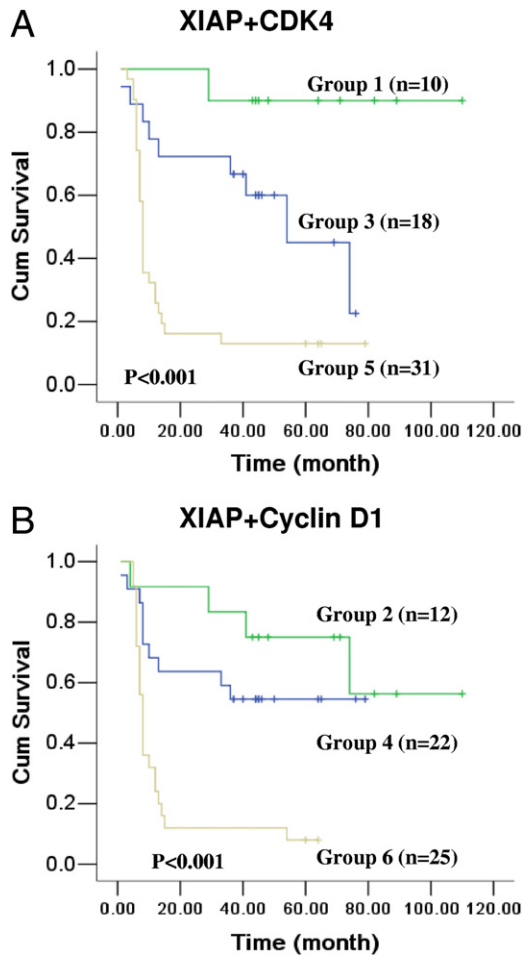


Figure 5. Co-expression of XIAP with CDK4 (A) and XIAP with Cyclin D1 (B) correlates with unfavorable survival. Overall survival rates of 59 HCC patients were compared among different groups. Group 1, low XIAP/low CDK4. Group 2, low XIAP/low Cyclin D1. Group 3, high XIAP/low CDK4 or low XIAP/high CDK4. Group 4, high XIAP/low Cyclin D1 or low XIAP/high Cyclin D1. Group 5, high XIAP/high CDK4. Group 6, high XIAP/high Cyclin D1.

these proteins as well as XIAP after treatment with embelin were examined. The results showed that Huh7 cells had a high level expression of XIAP, CDK4/6, and Cyclin D1 (Figure 9A), consistent with our findings in HCC tissues (Figure 2). Our results also showed that embelin significantly inhibited the expression of XIAP, CDK4/6, and Cyclin D1 in a dose-dependent manner (Figure 9A), suggesting that XIAP down-regulates CDK4/6 and Cyclin D1 expression, either directly or indirectly. These results support the notion that embelin causes G1 arrest via the down-regulation of CDK4/6 and Cyclin D1. It is interesting to note that embelin also inhibits XIAP expression, suggesting that embelin may have dual effects on XIAP, that is, direct inhibition and indirect down-regulation.⁸

To further determine the regulatory role of XIAP on CDK4/6 and Cyclin D1, siRNA specific to XIAP was transiently introduced into Huh 7 cells. The results showed that XIAP mRNA was efficiently reduced by siRNA (Figure 9B, top). Consequently, the protein levels of XIAP, CDK 4/6, and Cyclin D1 were also reduced (Figure 9B, bottom), suggesting that XIAP regulates the expression of CDK 4/6 and Cyclin D1. To further confirm this relation-

ship, the expression vector containing the XIAP gene was also introduced into Huh 7 cells. The results showed that the protein levels of CDK4/6 and Cyclin D1 were also increased (Figure 9C). Together, these results suggest that XIAP, either directly or indirectly, regulates the expression of CDK4/6 and Cyclin D1.

To understand the mechanism by which XIAP regulates CDK4/6 and Cyclin D1 expression, Huh 7 cells were treated either with 25 μ mol/L embelin or maintained without embelin for 24 hours, and the expression and phosphorylation of 137 proteins were examined using PPA. Our PPA results showed that, in addition to the above four proteins, 16 proteins had significant changes (>2-fold changes) in embelin-treated cells compared with controls. Of these proteins, 11 were upregulated in embelin-treated cells, including p-PTEN (6.72-fold), ER α (2.36), Twist (2.31), p-c-Jun (2.51), p27 (2.54), EGFR (2.12), TTF-1 (2.29), Notch4 (3.58), HIF3 α (3.85), IL1 β (2.08), and ERCC1 (2.13). In addition, five proteins were down-regulated, including CDC42 (-2.54-fold), H-Ras (-3.57), NF- κ B p65 (-2.16), PSM (-2.29), and RIP (-3.00). These results showed that embelin has broad effects on cell-regulatory proteins. These proteins were then put into the IPA to determine the interactive networks between them. After elimination of distant and indirect interactions among these proteins, five proteins, including NF- κ B p65, PTEN, RIP, JUN, and HRAS, were selected to generate a regulatory network between XIAP and Cyclin D1 and CDK4/6 (Figure 10).

Discussion

The scientific challenge to understanding HCC regulatory pathways come largely from the complex interactions between multiple molecular signals and pathways that often confound the eventual effect. Therefore, we took a different approach by examining the key regulatory proteins and pathways using our recently developed Protein Pathway Array technology.¹⁵ We initially screened 12 paired HCC and surrounding nontumor tissue resected from liver cancer using this technique. We found that 20 of 38 proteins and phosphoproteins were differentially expressed between benign and malignant tissues (>2-fold; Figure 2), suggesting a broad dysregulation of the signaling network in HCC. Among the altered proteins, XIAP, CDK4, CDK6, and Cyclin D1 were significantly overexpressed in HCC tissues, suggesting significant roles for these proteins in HCC development.

Inhibitors of apoptosis (IAPs) are crucial regulators in apoptosis and contain several RING finger and BIR domains.¹⁶ Among the IAPs, including XIAP, c-IAP1, and c-IAP2, XIAP is the most potent protein to inhibit the caspase cascade and suppress apoptosis.¹⁷ XIAP contains three BIR domains; the second BIR domain (BIR2) inhibits caspases 3 and 7, whereas the third BIR domain (BIR3) inhibits caspase 9 (1). Our results showed that overexpression of XIAP in HCC correlated with poor tumor differentiation (Table 1) and, more importantly, poor prognosis (Figure 4), consistent with a previous report.⁸

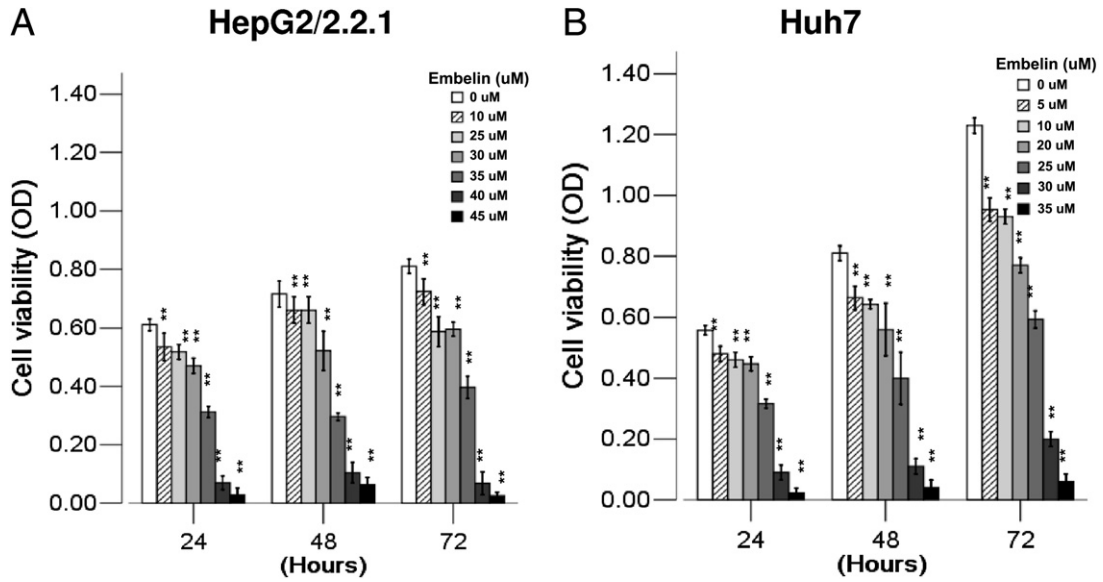


Figure 6. Inhibition of HCC cell growth by embelin. Both HepG2/2.2.1 (A) and Huh 7 (B) cells were treated with embelin at the concentrations and times indicated. There was a time- and dose-dependent inhibition of HCC cell growth. Results are expressed as the mean \pm SD of three independent studies. ** $P < 0.01$ compared with blank control.

Cell cycle progression is tightly regulated by protein complexes, including Cyclins and Cyclin-dependent kinases.¹⁸ The complex of Cyclin D1/CDK4/6, as well as Cyclin E/CDK2, sequentially phosphorylates the retinoblastoma protein (RB), which facilitates the G1-S transi-

tion.¹⁹ Our results show that increased expression of Cyclin D1 and CDK4 in HCC correlates with poor tumor differentiation, high TNM stages (Table 1), and poor prognosis (Figure 4). Interestingly, the level of Cyclin D1/CDK4 complex correlates with the level of XIAP in

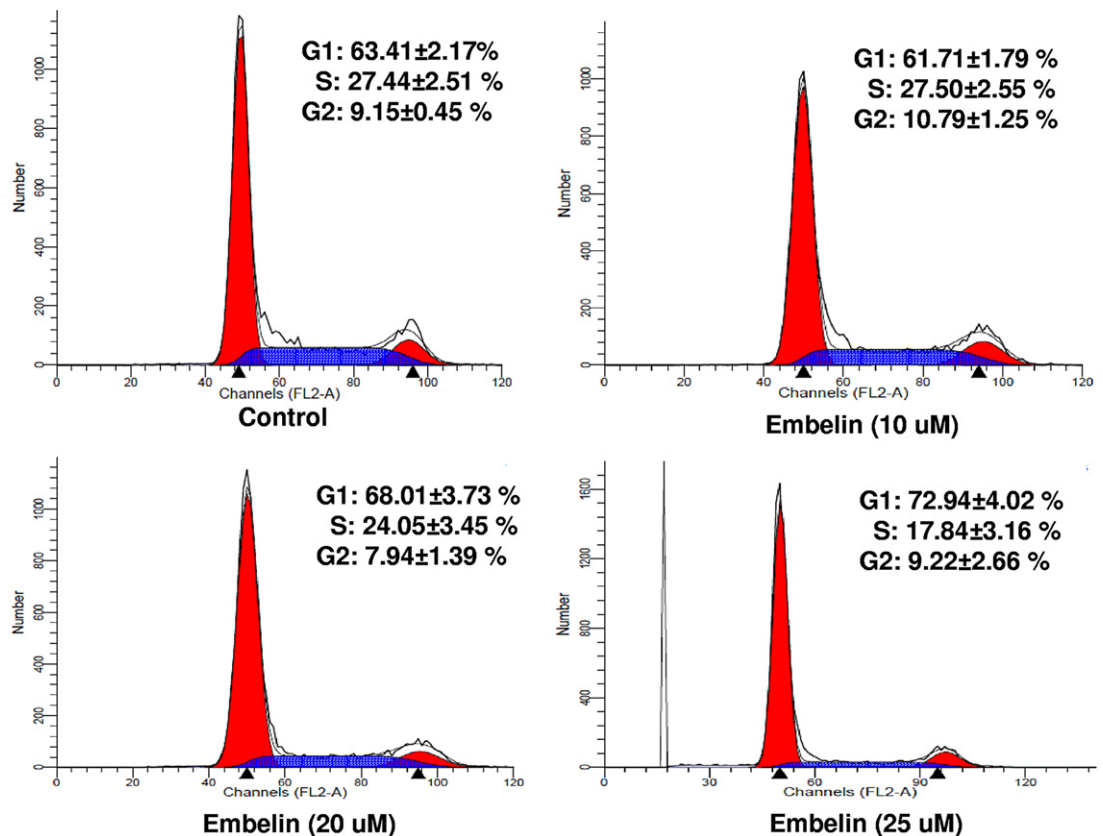


Figure 7. Effects of embelin on cell cycle distribution. Huh7 cells were treated with 10, 20, and 25 μ mol/L embelin for 24 hours, and both treated and untreated control cells were subjected to flow cytometry analysis. Representative graphs are presented. The values in the inset represent the mean \pm SD of three independent experiments.

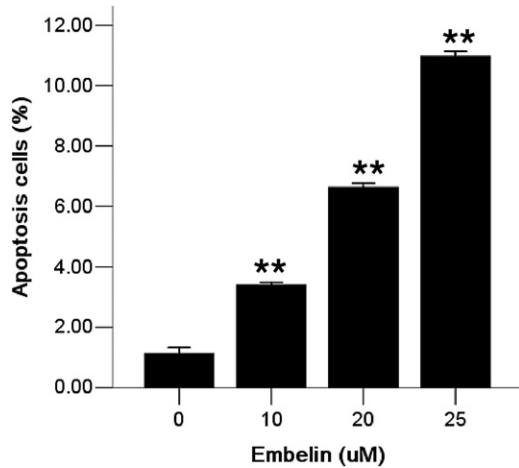


Figure 8. Effects of embelin on cell apoptosis. After treatment, cells were stained with Annexin V-FITC and propidium iodide and analyzed by flow cytometry. Results are shown as percentage of Annexin V-FITC-positive cells and represent the mean \pm SD of three independent experiments. ** $P < 0.01$ compared with blank control.

HCC. Moreover, co-expression of XIAP and Cyclin D1/CDK4 correlates with a poor prognosis in HCC patients (Figure 5). These data suggest a regulatory link between Cyclin D1/CDK4 and XIAP.

The role of XIAP in cell proliferation and apoptosis in HCC was further confirmed in our *in vitro* studies. Embelin is an XIAP-specific inhibitor that binds to the XIAP BIR3 domain, resulting in abrogation of the interaction between SMAC and XIAP BIR3 by displacing SMAC.²⁰ A recent study showed that high levels of XIAP in liver are necessary for FAS-induced apoptosis of hepatocytes, but not in other cells such as lymphocytes.²¹ Our results, as expected, showed a significant increase in the number of apoptotic cells after treatment with embelin (Figure 8). However, to our surprise, embelin also inhibits cell proliferation (Figure 6) by blocking cell progression at G1 phase (Figure 7). These results suggest that embelin exerts its effects on both apoptosis and cell cycle-related

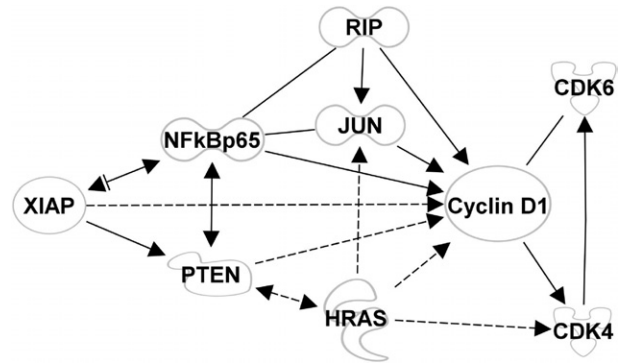


Figure 10. Proposed regulatory network between XIAP and Cyclin D1 and CDK4/6. A regulatory network was generated using IPA by inputting proteins that were altered by embelin. The network suggests that XIAP regulates Cyclin D1 and CDK4/6 expression via a complex network, primarily involving the NF- κ B and PTEN pathways. Solid lines indicate direct interactions. Dashed lines indicate indirect interactions. **Arrows** indicate stimulation.

pathways. To confirm these findings, we examined the expression of XIAP and cell cycle-related proteins, including XIAP, CDK4, CDK6, and Cyclin D1, after treatment with embelin. Our results demonstrated that embelin can inhibit the expression of these proteins (Figure 9), suggesting that XIAP regulates the expression of CDK4, CDK6, and Cyclin D1. This observation was further confirmed by our additional studies in which XIAP expression was either reduced by silencing or increased by expression vector (Figure 9). Taken together, our studies demonstrate that XIAP is a central regulator that bridges the apoptosis and cell cycle pathways in HCC.

Although the exact regulatory pathways between XIAP and Cyclin D1 and CDK4/6 are not clear, the IPA data suggest that a network of five proteins (ie, NF- κ B p65, PTEN, RIP, JUN, and HRAS) is involved in the regulation of Cyclin D1 and CDK4/CDK6 expression by XIAP (Figure 10). The data also suggest that XIAP directly interacts with the NF- κ B complex (a nuclear transcription factor consisting of subunits p50/52/65) and PTEN (phosphatase and tensin homolog, a tumor suppressor), which

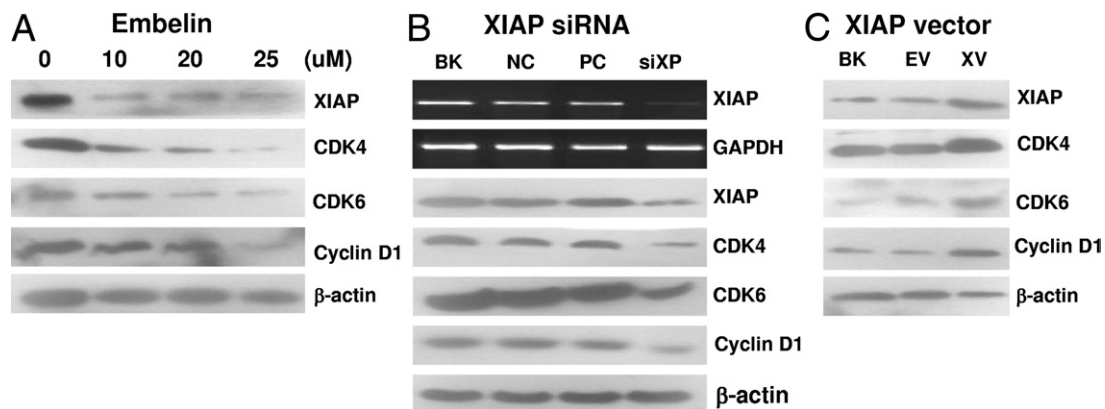


Figure 9. Effects of XIAP on CDK4/6 and Cyclin D1 expression. **A:** Huh 7 cells were treated with embelin at the concentrations indicated for 24 hours, and the protein levels of XIAP, CDK4/6, and Cyclin D1 were measured by Western blot. **B:** After Huh 7 cells were transfected with XIAP siRNAs for 72 hours, mRNA levels were analyzed by RT-PCR (top), and protein levels were analyzed by Western blot (bottom). BK, transfection reagent only; NC, Scramble RNA; PC, siRNA specific for GAPDH; siXP, siRNA specific for XIAP. **C:** Huh7 cells were transfected with Human pDsRed empty vector (EV) or Human pDsRed-XIAP expression vector (XV) for 48 hours. BK, transfection reagent only. Results showed a direct correlation between the level of XIAP and the expression of CDK4/6 and Cyclin D1. All experiments were repeated three times.

regulates proteins including RIP (nuclear receptor-interacting protein), JUN (c-Jun interacts with c-Fos to form AP-1 early response transcription factor), and HRAS (a GTPase responding to growth factor stimulation). These proteins, as well as XIAP, NF- κ B, and PTEN, then interact directly or indirectly with Cyclin D1, which then regulates CDK4/6. This complex interaction network may ensure the precise regulation of the expression of Cyclin D1 and CDK4/6 by XIAP. Several lines of evidence support this regulatory network. Recent reports showed that XIAP regulates ubiquitin (Ub)-dependent activation of IKK via its RING finger motif that then activates the NF- κ B transcription factors.²² Through the canonical and noncanonical signaling pathways, NF- κ B p65, as a transcription factor, drives the expression of many downstream genes including RIP, c-Jun, PTEN, and Cyclin D1. Yang et al reported that overexpression of NF- κ B p65 increased c-Jun mRNA levels and c-Jun-dependent promoter activity.²³ Both NF- κ B and AP-1 then regulate Cyclin D1 expression via the Cyclin D1 promoter region.^{24,25} A recent study also showed that inhibition of XIAP reduced proteasome-dependent degradation of PTEN via decreased ubiquitination.²⁶ It is of interest to note that a positive-feedback loop among Cyclin D1, CDK4, and CDK6 may further amplify the effects of XIAP on cell cycle regulation.

In conclusion, our results demonstrate the dysregulation of both apoptosis and cell cycle pathways in HCC and patients with XIAP, CDK4/6, and Cyclin D1 co-expression in their HCC carry a poor prognosis. XIAP is a key regulatory protein that communicates between apoptotic and cell proliferation pathways; therefore, it is a potential therapeutic target for HCC. Embelin is a specific XIAP inhibitor that could potentially be used in HCC treatment.

References

- Avila MA, Berasain C, Sangro B, Prieto J: New therapies for hepatocellular carcinoma. *Oncogene* 2006, 25:3866–3884
- Bosch FX, Ribes J, Diaz M, Cleries R: Primary liver cancer: worldwide incidence and trends. *Gastroenterology* 2004, 127:S5–S16
- Mann CD, Neal CP, Garcea G, Manson MM, Dennison AR, Berry DP: Prognostic molecular markers in hepatocellular carcinoma: a systematic review. *Eur J Cancer* 2007, 43:979–992
- Feng JT, Shang S, Beretta L: Proteomics for the early detection and treatment of hepatocellular carcinoma. *Oncogene* 2006, 25:3810–3817
- Pang RW, Poon RT: From molecular biology to targeted therapies for hepatocellular carcinoma: the future is now. *Oncology* 2007, 72(Suppl 1):30–44
- Villanueva A, Newell P, Chiang DY, Friedman SL, Llovet JM: Genomics and signaling pathways in hepatocellular carcinoma. *Semin Liver Dis* 2007, 27:55–76
- Li KK, Ng IO, Fan ST, Albrecht JH, Yamashita K, Poon RY: Activation of cyclin-dependent kinases CDC2 and CDK2 in hepatocellular carcinoma. *Liver* 2002, 22:259–268
- Shi YH, Ding WX, Zhou J, He JY, Xu Y, Gambotto AA, Rabinowich H, Fan J, Yin XM: Expression of X-linked inhibitor-of-apoptosis protein in hepatocellular carcinoma promotes metastasis and tumor recurrence. *Hepatology* 2008, 48:497–507
- Ye F, Che Y, McMillen E, Gorski J, Brodman D, Saw D, Jiang B, Zhang DY: The effect of *Scutellaria baicalensis* on the signaling network in hepatocellular carcinoma cells. *Nutr Cancer* 2009, 61:530–537
- Wang H, Gillis A, Zhao C, Lee E, Wu J, Zhang F, Ye F, Zhang DY: Crocidolite asbestos-induced signal pathway dysregulation in mesothelial cells. *Mutat Res* 2011, 723:171–176
- Wang X, Wang X, Gong W, Mi B, Liu S, Jiang B: Increased expression of beta-catenin, phosphorylated glycogen synthase kinase 3beta, cyclin D1, and c-myc in laterally spreading colorectal tumors. *J Histochem Cytochem* 2009, 57:363–371
- Lima RT, Martins LM, Guimaraes JE, Sambade C, Vasconcelos MH: Specific downregulation of bcl-2 and XIAP by RNAi enhances the effects of chemotherapeutic agents in MCF-7 human breast cancer cells. *Cancer Gene Ther* 2004, 11:309–316
- Cram EJ, Liu BD, Bjeldanes LF, Firestone GL: Indole-3-carbinol inhibits CDK6 expression in human MCF-7 breast cancer cells by disrupting Sp1 transcription factor interactions with a composite element in the CDK6 gene promoter. *J Biol Chem* 2001, 276:22332–22340
- Hasegawa T, Suzuki K, Sakamoto C, Ohta K, Nishiki S, Hino M, Tatsumi N, Kitagawa S: Expression of the inhibitor of apoptosis (IAP) family members in human neutrophils: up-regulation of cIAP2 by granulocyte colony-stimulating factor and overexpression of cIAP2 in chronic neutrophilic leukemia. *Blood* 2003, 101:1164–1171
- Zhang DY, Ye F, Gao L, Liu X, Zhao X, Che Y, Wang H, Wang L, Wu J, Song D, Liu W, Xu H, Jiang B, Zhang W, Wang J, Lee P: Proteomics, pathway array and signaling network-based medicine in cancer. *Cell Div* 2009, 4:20
- Zhang X, Dong N, Yin L, Cai N, Ma H, You J, Zhang H, Wang H, He R, Ye L: Hepatitis B virus X protein upregulates survivin expression in hepatoma tissues. *J Med Virol* 2005, 77:374–381
- Sakemi R, Yano H, Ogasawara S, Akiba J, Nakashima O, Fukahori S, Sata M, Kojiro M: X-linked inhibitor of apoptosis (XIAP) and XIAP-associated factor-1 expressions and their relationship to apoptosis in human hepatocellular carcinoma and non-cancerous liver tissues. *Oncol Rep* 2007, 18:65–70
- Sausville EA: Complexities in the development of cyclin-dependent kinase inhibitor drugs. *Trends Mol Med* 2002, 8:S32–S37
- Sherr CJ: G1 phase progression: cycling on cue. *Cell* 1994, 79:551–555
- Nikolovska-Coleska Z, Xu L, Hu Z, Tomita Y, Li P, Roller PP, Wang R, Fang X, Guo R, Zhang M, Lippman ME, Yang D, Wang S: Discovery of embelin as a cell-permeable, small-molecular weight inhibitor of XIAP through structure-based computational screening of a traditional herbal medicine three-dimensional structure database. *J Med Chem* 2004, 47:2430–2440
- Jost PJ, Grabow S, Gray D, McKenzie MD, Nachbur U, Huang DC, Bouillet P, Thomas HE, Borner C, Silke J, Strasser A, Kaufmann T: XIAP discriminates between type I and type II FAS-induced apoptosis. *Nature* 2009, 460:1035–1039
- Gyrd-Hansen M, Meier P: IAPs: from caspase inhibitors to modulators of NF-kappaB, inflammation and cancer. *Nat Rev Cancer* 2010, 10:561–574
- Yang H, Magilnick N, Ou X, Lu SC: Tumour necrosis factor alpha induces co-ordinated activation of rat GSH synthetic enzymes via nuclear factor kappaB and activator protein-1. *Biochem J* 2005, 391:399–408
- Joyce D, Albanese C, Steer J, Fu M, Bouzahzah B, Pestell RG: NF-kappaB and cell-cycle regulation: the cyclin coin. *Cytokine Growth Factor Rev* 2001, 12:73–90
- Bakiri L, Lallemand D, Bossy-Wetzel E, Yaniv M: Cell cycle-dependent variations in c-Jun and JunB phosphorylation: a role in the control of cyclin D1 expression. *EMBO J* 2000, 19:2056–2068
- Van Themsche C, Leblanc V, Parent S, Asselin E: X-linked inhibitor of apoptosis protein (XIAP) regulates PTEN ubiquitination, content, and compartmentalization. *J Biol Chem* 2009, 284:20462–20466